ELSEVIER

Nuclear Physics A588 (1995) 191c–196c

NUCLEAR PHYSICS A

Production, identifiife and halflife measurement of ^{100}Sn*

R. Schneider[a], T. Faestermann[a], J. Friese[a], R. Gernhäuser[a], H. Geissel[b], H. Gilg[a], F. Heine[a], J. Homolka[a], P. Kienle[a], H.-J. Körner[a], G. Münzenberg[b], J. Reinhold[a], K. Sümmerer[b], and K. Zeitelhack[a]

[a]Physik-Department E12, Technische Universität München, D-85747 Garching, Germany

[b]Gesellschaft für Schwerionenforschung, P.O. Box 110552, D-64220 Darmstadt, Germany

We report the first observation of the doubly-magic nucleus ^{100}Sn. The isotope was produced by nuclear fragmentation of ^{124}Xe projectiles at 1095 A·MeV using the heavy-ion synchrotron SIS at GSI Darmstadt. The projectile fragments were separated in flight with the projectile-fragment separator FRS and identified by measuring event by event the magnetic rigidity, the time of flight and the energy deposition. After identification the ions were implanted into a silicon detector stack and the decay was studied. We report preliminary results of the halflife determination.

1. INTRODUCTION

The region of isotopes around doubly-magic nuclei has always been an important testing ground for the nuclear shell model. Of particular interest are the N=Z doubly-magic nuclei, with ^{100}Sn being the heaviest nucleus that is expected to be stable against ground-state proton emission. Despite large experimental efforts ^{100}Sn remained undiscovered. The lightest tin isotopes studied so far were ^{103}Sn [1], [2] and ^{101}Sn [3]. In both cases the observation was facilitated by the beta-delayed proton decay of these isotopes, whereas for ^{100}Sn a pure β-decay is expected [4]. For even–even neighbouring nuclei a hindrance of the Gamow–Teller transition by a factor ~ 4 has been observed [5]. However, those nuclei have in general a more complicated multiparticle-multihole configuration.The study of the decay properties of ^{100}Sn allows one to investigate the GT strength for the pure single-particle transition from a proton in the filled $g_{9/2}$ shell to a $\pi g_{9/2}^{-1} \otimes \nu g_{7/2}^{1}$ particle-hole state. In our experiment ^{100}Sn was observed in the fragmentation of ^{124}Xe projectiles [6] and first preliminary data obtained of the decay characteristics are available.

2. FRAGMENTATION OF XENON ISOTOPES

Systematic studies of high-energy projectile fragmentation with different xenon isotopes suggested the possibility to produce ^{100}Sn by using this technique. Fig. 1 shows a comparison of the fragmentation of ^{129}Xe projectiles on an aluminum target [7] with

*This work has been partially funded by the German Federal Minister for Research and Technology (BMFT) under contract number 06TM353 TP1.

SSDI 0375-9474(95)00138-7

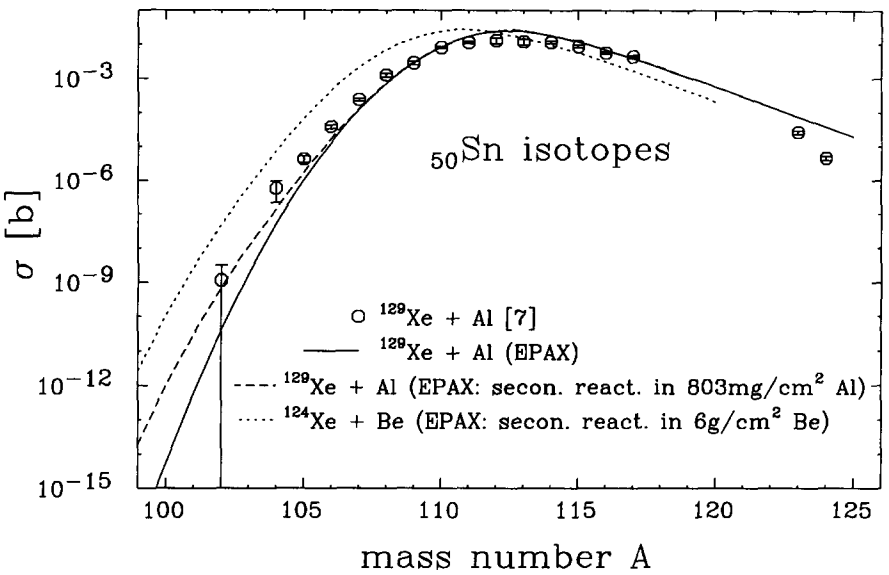

Figure 1. Production cross sections of tin isotopes from the fragmentation of various xenon projectiles. Symbols are data, lines are EPAX [8] parametrization.

the prediction of an empirical parametrization (EPAX) [8]. EPAX accounts for a shift of the projectiles mass-to-charge ratio with respect to the general trend of the line of β-stability ("memory-effect"). This effect has been verified for neutron rich projectiles in the fragmentation of ^{136}Xe [9] on an aluminum target.

The tin isotope distribution for the ^{129}Xe projectile is reproduced by EPAX within an overall accuracy of a factor two [8]. However there are indications for the very neutron deficient isotopes close to the proton-drip line, that the cross sections might be much larger than predicted by the parametrization. A similar behaviour was also observed in the fragmentation of ^{58}Ni [10] projectiles. Partly this can be explained by a possible contribution of secondary reactions to the observed yield of a certain isotope. Heavier fragments with mass and charge greater than that of the isotope of interest can undergo a second reaction in a thick target and thus simulate higher cross sections. This is shown in Fig. 1 with the dashed line, taking into account all possible intermediate fragments with $A_{final} \leq A_{interm.} \leq A_{proj}$ and $Z_{final} \leq Z_{interm.} \leq Z_{proj}$ and by using the corresponding EPAX cross sections for fragment production. The calculated enhancement is mainly due to the strong "memory effect" assumed by EPAX for the very neutron deficient intermediate fragments. For ^{124}Xe, the most neutron deficient stable xenon isotope, the expected yield is about two ^{100}Sn nuclei per 10^{11} projectiles in a 6g/cm^2 beryllium target (dotted line in Fig. 1). Because of fewer possible intermediate fragments such an enhancement due to secondary reactions is not expected for ^{112}Sn projectiles. Therefore ^{124}Xe was choosen as a projectile.

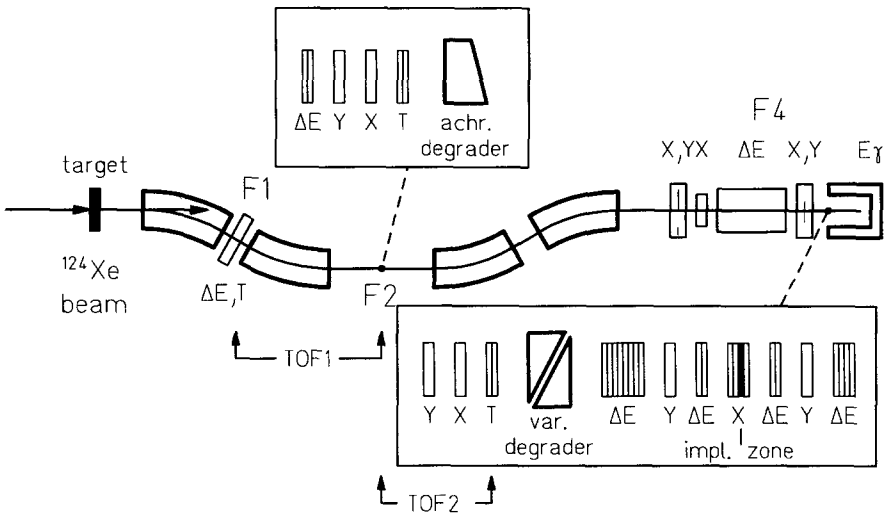

Figure 2. Experimental setup used for the separation and identification of ^{100}Sn and neighbouring isotopes at the fragment separator FRS.

3. EXPERIMENTAL SETUP

A ^{124}Xe beam was accelerated in the UNILAC and the SIS heavy-ion synchrotron at GSI to an energy of 1095 A·MeV. Spills with a length of two seconds and an average number of 10^8 ions were extracted every five seconds and directed onto a 6g/cm^2 beryllium target in front of the fragment separator FRS [11]. A schematic layout of the FRS and the detectors used to identify the fragments and measure their decay is shown in Fig. 2. The separator was operated with an achromatic focus at F4 and a thick wedge-shaped aluminum degrader (6.3g/cm^2) in the dispersive midplane F2 to achieve isotopic separation. Several detector systems were mounted in the focal planes F1, F2, and F4. Silicon strip detectors at F2 and F4, and two large-area multi-wire proportional counters at F4 served to determine the fragments magnetic rigidity $B\rho = (M/Q)\gamma v$ by measuring their position. Multiple time-of-flight measurements with silicon detectors thus allowed to determine the fragments mass-to-charge ratio M/Q. As at this energy the fragments are fully ionized [12], the charge Q can be substituted by the nuclear charge Ze. An independent measurement of the nuclear charge by energy deposition measurements in silicon detectors and an ionization chamber therefore leads to an unambiguous isotope identification. After identification the ions were slowed down in a degrader of variable thickness and by a stack of silicon detectors. Finally they were implanted into a stack of position sensitive silicon strip detectors. The detector system in front of the strip detectors and a second stack at the back allowed to detect beta particles in nearly 4π geometry. The complete implantation detector setup was surrounded by a large BGO crystal in order to detect gamma rays and annihilation radiation.

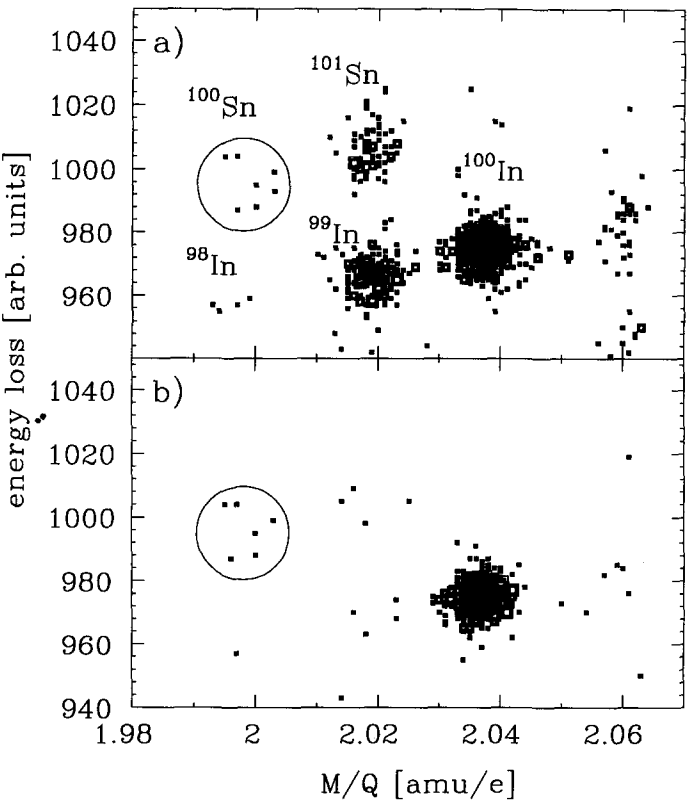

Figure 3. Energy-deposition vs. mass-to-charge ratio measured in the final focal plane F4 of the FRS. The field setting corresponds to the magnetic rigidity of ^{100}Sn.
a): all fragments transmitted to F4 ($\Delta x \cdot \Delta y = 150 \cdot 20mm^2$).
b): fragments transmitted to the implantation detector system ($\Delta x \cdot \Delta y = 50 \cdot 20mm^2$).

4. IDENTIFICATION

Fig. 3 shows the measured energy deposition in an ionization chamber at F4 versus the mass-to-charge ratio M/Q extracted from the time-of-flight and magnetic rigidity measurement from F2 to F4 ("TOF2"). The spectrum was obtained with a FRS field setting optimized for the detection of the isotope ^{100}Sn. Fig. 3a shows all fragments that were transmitted to the final focal plane F4 with an acceptance area of 15cm times 2cm. The individual isotopes are clearly resolved. The 7 events at a mass-to-charge ratio of M/Q=2.0 and an energy of $\Delta E \approx 990$ (arbitrary units) are attributed to the isotope ^{100}Sn. In Fig. 3b only those ions are shown, that were transmitted through the aperture (-2cm<x<+2cm) of an 18cm thick lead absorber at F4 into the implantation detector system. The number of counts for the isotopes ^{100}Sn and ^{100}In remain nearly unaltered,

Table 1
Decay events following the implantation of ^{100}Sn nuclei in the Si-strip detector

event	β-energy	measured decay times [s]		
#	of ^{100}Sn [MeV]	^{100}Sn	^{100}In ($\tau = 9s$)	^{100}Cd ($\tau = 90s$)
1	0.7	0.716	6.6	
2	1.6	1.208		36
3	1.4	1.219	13.3	35
4	2.7	0.655		69
5				26
6	1.5	0.98		
7	1.6	3.02	9.1	

whereas the number of ^{101}Sn and ^{99}In are reduced by roughly a factor 10. This reflects the separation characteristics of the FRS as expected from ion-optical calculations. We conclude that the observed events for ^{100}Sn do not originate from the tails of the more abundant neighbouring isotope distributions. One of the seven ^{100}Sn isotopes shown in Fig. 3a is lost, because it missed the aperture in front of the implantation detector by a few mm. The present state of the analysis attributes two additional events to the isotope ^{100}Sn, not shown in Fig. 3. So, altogether 9 isotopes ^{100}Sn were identified with 7 of them implanted into the final detector system. These are used for further decay measurements.

5. DECAY

For the seven ^{100}Sn isotopes that were implanted into the final detector system a first analysis of subsequent decay events was performed. The total efficiency to detect a decay event was $\epsilon \approx 65\%$ (detector efficiency and deadtime). The results are summerized in Table 1. All measured decay events were identified as β-decays. Also some subsequent decays from the daughter ^{100}In and/or the granddaughter ^{100}Cd could be detected. The random background rate in the corresponding detectors were $1/230s^{-1}$ for the events numbered 1-4 in Table 1 and $1/15s^{-1}$ for the events numbered 5-7. Therefore only event number 1-4 were used for a preliminary estimation of the halflife. We deduce for ^{100}Sn a halflife of $T_{1/2} = 0.66^{+0.59}_{-0.22}s$. The errors were calculated as described in [13].

6. SUMMARY

Although the observed yield for the isotope ^{100}Sn does not meet the expectations, the excellent separation characteristic of the FRS together with the high granularity of the implantation detector allowed to identify and measure the decay of ^{100}Sn for the first time. During the experiment several other isotopes in the vicinity of ^{100}Sn could be produced with yields sufficient to perform more detailed decay studies. These results are summerized in Table 2 and will be discussed in more detail elsewhere [14].

A preliminary estimate of the production cross sections indicates that the "memory effect" — observed for fragments closer to β-stability — appears to vanish close to the proton-drip line. Although secondary reactions have to occur in a thick target, the EPAX

Table 2
Preliminary measured decay characteristics of isotopes in the vicinity of ^{100}Sn.

isotope	$t_{1/2}$ [s]	decay counts	decay mode	beam time
^{108}Te	2.0 ± 0.26	61	β^+, α	2h
^{105}Sb	1.3 ± 0.15	73	β^+, p?	3.5h
^{104}Sb	$0.52^{+0.18}_{-0.13}$	13	β^+, p/$\beta^+ < 8\%$	8h
^{102}Sn	4.5 ± 0.7	43	β^+	35
^{100}Sn	$0.66^{+0.59}_{-0.22}$	4	β^+	300h

approach to handle the "memory effect" does not appear to be suited to decribe either the very neutron deficient tail of the isotopic distributions nor the "memory effect" for very neutron deficient projectiles. As a consequence also ^{112}Sn has to be considered as suitable projectile for further experiments. Almost simultaneously with our discovery, ^{100}Sn has been observed at the LISE separator at GANIL, using intermediate-energy projectile-fragmentation of 58 A·MeV ^{112}Sn [15]. Since at lower energies the coexistence of several ionic chargestates complicates the fragment identification and leads to low transmission, it is necessary to test whether the high-energy projectile-fragmentation of ^{112}Sn yields comparable or even higher production rates.

The authors thank K.-H. Behr, A. Brünle, K. Burkard, W. Czech, H. Falkner, M. Klöckner, R. Lang, E. Pfeng, and S. Winkler for technical support. We gratefully acknowledge the contributions of all our colleagues at the FRS to the excellent performance of the separator. We are indebted to the GSI accelerator staff for providing intense beams of ^{124}Xe and to the GSI target laboratory for preparing high-quality targets and degraders.

REFERENCES

1. P. Tidemand-Petersson et al., Z. Physik A302 (1981) 343.
2. Z. Janas et al. GSI-Preprint 94-47, to be published in Physica Scripta.
3. J. Szerypo et al., Preprint GSI–94–38 (1994)
4. B.A. Brown and K. Rykaczewski, to be published in Phys. Rev. Lett.
5. K. Rykaczewski, Proc. 6^{th} Int. Conf. on Nuclei far from Stability, Bernkastel-Kues, Germany, 1992, IOP Conference Series 132 (IOP Publishing, Bristol, 1993) p. 517.
6. R. Schneider et al., Z. Phys. A348 (1994) 241.
7. J. Friese et al., Proceedings of the 9th High Energy Heavy Ion Study, October 25-29, 1993, LBL, University of California, Berkeley, California, LBL-35984.
8. K. Sümmerer et al., Phys. Rev. C42 (1990) 2546.
9. J. Friese et al., Nucl. Phys. A553 (1993) 753c.
10. B. Blank et al., Phys. Rev. C50 (1994) 2398.
11. H. Geissel et al., Nucl. Instr. Meth. B70 (1992) 286.
12. Th. Stöhlker et al., Nucl. Instr. Meth. B61 (1991) 408.
13. K.H. Schmidt et al., Z. Phys. A316 (1984) 19.
14. R. Schneider et al., Proceedings to SELMA 1994, to be published in Physica Scripta.
15. M. Lewitowicz et al., Phys. Lett. B332 (1994) 20.